NASA CR-178,484

NASA CONTRACTOR
REPORT

NASA CR-178484

CONFINED SWIRLING JET PREDICTIONS USING A MULTIPLE-SCALE TURBULENCE MODEL

By C. P. Chen
Resident Research Associate
National Research Council
Science and Engineering Directorate
Systems Dynamics Laboratory

Interim Report

August 1985

Prepared for
NASA-Marshall Space Flight Center
Marshall Space Flight Center, Alabama 35812

TECHNICAL REPORT STANDARD TITLE PAGE

1. REPORT NO.	2. GOVERNMENT ACCESSION NO.	3. RECIPIENT'S CATALOG NO.
NASA CR-178484		

4. TITLE AND SUBTITLE	5. REPORT DATE
Confined Swirling Jet Predictions Using a Multiple-Scale Turbulence Model	August 1985
	6. PERFORMING ORGANIZATION CODE
7. AUTHOR(S)	8. PERFORMING ORGANIZATION REPORT #
*C. P. Chen	
9. PERFORMING ORGANIZATION NAME AND ADDRESS	10. WORK UNIT NO.
George C. Marshall Space Flight Center Marshall Space Flight Center, Alabama 35812	11. CONTRACT OR GRANT NO. NASW-3458
	13. TYPE OF REPORT & PERIOD COVERED
12. SPONSORING AGENCY NAME AND ADDRESS	Contractor Report
National Aeronautics and Space Administration Washington, D.C. 20546	14. SPONSORING AGENCY CODE

15. SUPPLEMENTARY NOTES

Prepared by Systems Dynamics Laboratory, Science and Engineering Directorate.
*National Research Council

16. ABSTRACT

In this study, a recently developed multiple-scale turbulence model is used for the numerical prediction of isothermal, confined turbulent swirling flows. Because of the streamline curvature and non-equilibrium spectral energy transfer nature of the swirling flow, the utilized multiple-scale turbulence model includes a different set of response equations for each of the large-scale energetic eddies and the small-scale transfer eddies. Predictions are made of a confined coaxial swirling jet in a sudden expansion and comparisons are made with experimental data and with the conventional single-scale two-equation model. The multiple-scale model shows significant improvement of predictions of swirling flows over the single-scale k-ε model. The sensitivity study of the effect of prescribed inlet turbulence levels on the flow fields is also included.

17. KEY WORDS	18. DISTRIBUTION STATEMENT
Turbulence Swirl Modeling Recirculating	Unclassified — Unlimited

19. SECURITY CLASSIF. (of this report)	20. SECURITY CLASSIF. (of this page)	21. NO. OF PAGES	22. PRICE
Unclassified	Unclassified	21	NTIS

MSFC - Form 3292 (May 1969)

For sale by National Technical Information Service, Springfield, Virginia 22151

ACKNOWLEDGMENTS

This work was done while the author held a National Research Council-NASA Research Associateship. Financial support provided by NASA-MSFC and NRC is acknowledged.

TABLE OF CONTENTS

LIST OF ILLUSTRATIONS

CONTRACTOR REPORT

CONFINED SWIRLING JET PREDICTIONS USING A MULTIPLE-SCALE TURBULENCE MODEL

I. INTRODUCTION

Confined jets are encountered in many types of engineering equipment such as coal gasifier, aircraft gas turbine engine, and ramjet combustors. Swirl is often introduced to control the mixing of fuel and oxidizer, flame size, and combustion intensities. Thus, it is important to be able to predict the flow structure in terms of effects of geometric configuration of the combustor, turbulence intensities of inlet stream, and swirl strength.

In the last decade, advances have been made in turbulence modeling such that it is possible to predict certain mean and turbulence characteristics of many flows. Among the models, the so-called k-ε model has been shown to be adequate in a variety of flows [1]. However, in complex flows such as confined swirling flows, k-ε models are known to be deficient [2] due to the neglect of anisotropy in the turbulent viscosity and additional turbulence generation arising from streamline curvature. Several proposals have been raised in the last few years trying to remedy this defect. Specifically, a variant in the k-ε model is to modify the sink or source term in the ε-equation by introducing a gradient Richardson number [3] or a flux Richardson number [4] to account for the swirl-induced streamline curvature effect. Although the detailed interpretation of these two Richardson numbers is different, both modifications assume that the turbulence amplification effect of swirl can be modeled due to the changes in the large scale of energetic eddies. In other words, these modifications assume that there exists a constant energy transfer rate through the energy spectrum and that a single velocity and length scale can be used to characterize the whole spectrum of turbulence motion. This is thought to be conceptually weak because the flow field in a confined vortex tube is not in spectral equilibrium due to swirl induced destabilizing effects. This also tends to explain why these two modifications, and several other modifications developed on similar reasoning, only give improvements of the predictions in certain regions of the swirling flow [5,6].

To circumvent this defect, a so-called "multiple-scale" turbulence model is used in the present report to study the confined swirling flows. A basic feature of this model is the partition of energy spectrum. This would allow the energy transfer of energetic vortexes to be modeled based on the properties of the large scale turbulence, such as mean velocity gradients and degree of swirl, while the dissipation rate is related to the energy transfer by its own action rather than to the overall kinetic energy.

In section II, a brief description of this multiple-scale turbulence model will be given and numerical results of a specific confined swirling jet will be presented in section III. One major effort of this study is to test the validity of the multiple-scale turbulence model by predicting the confined swirling jet. These studies will form a basis for multiple-phase closure models.

II. ANALYSIS

A. The Mean Governing Equations

Introducing the gradient-diffusion Boussinesq type approximation into the mean Reynolds equation for conservation of momentum, the transport equations can be cast into the standard form [7] (cylindrical coordinates):

$$\frac{\partial}{\partial x}(\rho U\phi) + \frac{1}{r}\frac{\partial}{\partial r}(r\rho V\phi) - \frac{\partial}{\partial x}\left(\Gamma_\phi \frac{\partial \phi}{\partial x}\right) - \frac{1}{r}\frac{\partial}{\partial r}\left(r\Gamma_\phi \frac{\partial \phi}{\partial r}\right) = S_\phi \tag{1}$$

where ϕ is dependent variable, $\phi = 1$ for mass conservation, and $\phi = U,V,W$, for three velocity components, S_ϕ is the comprehensive source term, and Γ_ϕ is the phenomenological exchange coefficient. Source terms S_ϕ for these mean quantities can be found in Reference 7 and thus are not repeated here.

B. Turbulence Model

Turbulence effects which enter the mean governing equations are modeled through gradient-type approximation. The eddy viscosity ν_t is represented by the so-called multiple-scale turbulence model [8,9]. This model includes a different set of response equations for each of the large-scale energetic eddies and the dissipative eddies. The balance equations for the energy and dissipation rate of large-scale vortexes and small-scale eddies are derived separately. Specifically, two transport equations are provided representing the evolution of turbulent energy associated with each of the production range of the energy spectrum k_p and transfer region of the energy spectrum k_t. To close these equations, two transport equations for the energy dissipation rate are derived. The dissipation of the energetic eddies, ε_p, can be interpreted as the energy transfer rate from the energy-containing eddy motions. On the other hand, the dissipation rate of the small eddies, ε_t, is related to the energy transferred by its own action in the high wave number region of the spectrum. These transport equations are:

$$\frac{\partial U k_p}{\partial x} + \frac{1}{r}\frac{\partial}{\partial r}(r\,V\,k_p) = \frac{\partial}{\partial x}\left(\frac{\nu_t}{\sigma_{k_p}}\frac{\partial k_p}{\partial x}\right) + \frac{1}{r}\frac{\partial}{\partial r}\left(\frac{r\,\nu_t}{\sigma_{k_p}}\frac{\partial k_p}{\partial r}\right) + G - \varepsilon_p \tag{2}$$

$$\frac{\partial U k_t}{\partial x} + \frac{1}{r}\frac{\partial}{\partial r}(r\,V\,k_t) = \frac{\partial}{\partial x}\left(\frac{\nu_t}{\sigma_{k_t}}\frac{\partial k_t}{\partial x}\right) + \frac{1}{r}\frac{\partial}{\partial r}\left(\frac{\nu_t}{\sigma_{k_t}}\frac{\partial k_t}{\partial r}\right) + \varepsilon_p - \varepsilon_t \tag{3}$$

$$\frac{\partial U \varepsilon_p}{\partial x} + \frac{1}{r}\frac{\partial}{\partial r}(r\,V\,\varepsilon_p) = \frac{\partial}{\partial x}\left(\frac{\nu_t}{\sigma_{\varepsilon_p}}\frac{\partial \varepsilon_p}{\partial x}\right) + \frac{1}{r}\frac{\partial}{\partial r}\left(r\frac{\nu_t}{\sigma_{\varepsilon_p}}\frac{\partial \varepsilon_p}{\partial r}\right) + \frac{1}{\tau_p}\left[C_{p_1} G - C_{p_2} \varepsilon_p\right] \tag{4}$$

$$\frac{\partial U \varepsilon_t}{\partial x} + \frac{1}{r}\frac{\partial}{\partial r}(r V \varepsilon_t) = \frac{\partial}{\partial x}\left(\frac{\nu_t}{\sigma_{\varepsilon_t}}\frac{\partial \varepsilon_t}{\partial x}\right) + \frac{1}{r}\frac{\partial}{\partial r}\left(r\frac{\nu_t}{\sigma_{\varepsilon_t}}\frac{\partial \varepsilon_t}{\partial r}\right) + \frac{1}{\tau_p}[C_{t_1}\varepsilon_p - C_{t_2}\varepsilon_t] \tag{5}$$

where

$$G \equiv \nu_t \left\{ 2\left[\left(\frac{\partial U}{\partial x}\right)^2 + \left(\frac{\partial V}{\partial r}\right)^2 + \left(\frac{V}{r}\right)^2\right] + \left(\frac{\partial U}{\partial r} + \frac{\partial V}{\partial x}\right)^2 + \left(\frac{\partial W}{\partial x}\right)^2 + \left[r\frac{\partial}{\partial r}\left(\frac{W}{r}\right)^2\right]\right\}$$

is the production of energy-containing eddies by the mean gradients and $\tau_p = k_p/\varepsilon_p$. Note that the time scale used in equation (5) is different from the one used in Reference 8.

This version of multiple-scale model was developed based on the earlier version of Hanjalic et al. [8] and has been tested on several confined recirculating flows [9]. The details of the model development can be found in these two papers. The modeled coefficients in the turbulence model are established guided by Reference 8 and are detailed in Reference 9. These are:

$$\sigma_{k_p} = \sigma_{k_t} = 1 \quad ,$$

$$\sigma_{\varepsilon_p} = \sigma_{\varepsilon_t} = 1.22 \quad ,$$

$$C_{p_1} = 1.6 \quad , \quad C_{p_2} = 1.8 - 0.3\frac{[1 - k_t/k_p]}{[1 + k_t/k_p]}$$

$$C_{t_1} = 1.15 \quad , \quad C_{t_2} = 1.8\frac{\varepsilon_t}{\varepsilon_p} \quad .$$

Using these model equations, the Reynolds stresses are expressed according to

$$\overline{u_i' u_j'} = -\nu_t\left[\frac{1}{2}\left(\frac{\partial U_i}{\partial x_j} + \frac{\partial U_j}{\partial x_i}\right)\right] + \frac{2}{3} k \delta_{ij} \tag{6}$$

where

$$k = k_t + k_p$$

and the eddy viscosity is given by

$$\nu_t = C_\mu (k_p + k_t)\frac{k_p}{\varepsilon_p} \qquad \text{with } C_\mu = 0.09 \quad . \tag{7}$$

C. Boundary Conditions

The experimental work used to evaluate the turbulence model is a confined coaxial jet involving sudden expansion with swirl in the annular jet by Roback and Johnson [10]. The annular swirling flow was generated by a 30 deg, free vortex swirler. The elliptic numerical procedure used for solution requires prescriptions of all boundary conditions of the solution domain. Specification of the inlet plane boundary conditions require special attention because these conditions have a crucial effect on the flow field calculated downstream [11-14]. Ideally, inlet conditions should be supplied from the experimental data, in this case, at the expansion plane. Unfortunately the measurements were not performed by Roback and Johnson at this plane due to optical difficulties. Calculation starting at the plane upstream of the expansion is also unfeasible because the flow field generated from the fluid passing through swirl-vanes, is highly complex and three dimensional. Following Leschziner and Rodi [11], the computation domain thus starts at the first experimentally measured plane which lies just downstream of the expansion at $X/D \sim 0.04$ (D is the diameter of the confined chamber). Distributions of U, V, W and k were available, however ε was not. Thus, ε is estimated from the measured $\overline{u_i' u_j'}$ through the standard k-ε model relationship:

$$\varepsilon = -C_\mu \frac{k^2}{\rho \overline{u_i' u_j'}} \frac{\partial U_i}{\partial x_j} \quad . \tag{8}$$

These two turbulence quantities, k and ε, are then used to estimate the inlet profiles for multiple-scale turbulence quantities. In this plane the flow is assumed to be highly non-equilibrium, thus the non-equilibrium conditions are applied. This implied [9]

$$k_p = k_t = \frac{1}{2} k$$

and

$$\varepsilon_p = 0.5\ \varepsilon_t = \varepsilon \quad .$$

Along the solid wall, the dependent variables are matched to the usual "wall functions" and equivalent local-equilibrium expressions for the turbulence quantities. Specifically, the near wall energy transfer rates ε_p and ε_t are set equal to one another. A symmetric axis was specified where the radial velocity and radial gradients of all other variables were set to zero except near the axis where W was deduced from solid body rotation by assuming W to be zero on the axis.

III. NUMERICAL RESULTS AND DISCUSSION

Numerical solutions were obtained with a modified version of the TEACH-T computer code of Gosman and Iderah [15]. The numerical procedure is developed

based on finite-volume formulation with hybrid upwind/central-difference scheme for convection terms. The computations are made on a 45 x 35 non-uniform mesh with concentrations of nodes in the recirculation regions, in the entrance region, and near wall regions. Solutions with this mesh were found to be nearly grid-independent [5].

When swirl is introduced in the annular flow of a confined coaxial jet, significant radial and axial pressure gradients are set up near the central jet exit. At high degrees of swirl (swirl number $\gtrsim 0.5$), given the geometry of the enclosure chamber and design of swirl vanes, a central recirculation zone will form. The types of recirculation can be of shape characterized by a large central reverse-flow zone (Type 2) or of shape characterized by an annular zone of recirculation (Type 1) or some combination of both (Type 3) depending on the mass flux ratio of annular jet to central jet [16]. The comparison of the predictions and experiments will be first made on the global features of the flow field.

One of the important parameters to compare in confined flows is the corner reattachment length. This length, reported by Roback and Johnson, is approximately 50 mm which is about one-third the length observed with non-swirling case for the same flow condition. Presented in Table 1 is the prediction of this length by multiple-scale and single-scale k-ε models. Two corrections of the k-ε model mentioned in Reference 5 are also included. It can be seen that this length is reduced by about 10 percent between the single-scale and multiple-scale turbulence model and that the magnitude of this length is correctly predicted by the multiple-scale turbulence model.

TABLE 1. COMPARISON OF CORNER RECIRCULATION ZONE LENGTH

Model	Reattachment Length (mm)
k-ε	$\sim$77
Launder et al.	$\sim$80
Rodi	$\sim$70
Multiple-scale	$\sim$55
Experiment	$\sim$50

Figure 1 shows comparisons of axial velocities along the centerline using k-ε model and multiple-scale model. It can be seen that the multiple-scale model improves the prediction of the strength of the recirculation and predicts a faster recovery of the flow than the k-ε model downstream of the central recirculation region. Figure 2 is taken from the previous study [5] of comparison of two k-ε model corrections. Based on the analysis discussed in Reference 5, the multiple-scale model suppresses the diffusion process, thus giving stabilizing effects in the central recirculation region. On the other hand, it serves to destabilize the turbulence and speeds up the recovery of the centerline velocity to its asymptotic value after the recirculation region. The implication is that the multiple-scale turbulence model relates the energy transfer rate depending on swirl impartation and flow structure. In the central recirculation region, the k-ε model tends to connect the energy transfer rate to the local mean strain rate too strongly. The multiple-scale model suppresses this tendency. However, further downstream of the recirculation zone, where the velocity gradient is small, since the energy transfer rate of the transfer range eddies does

not depend on the mean flow structure [equation (3,5)], multiple-scale model persists on the diffusion process, thus enhances the recovery of the flow.

This behavior can be observed in Figures 3 and 4. Radial profiles of axial velocities are plotted at X/D = 0.833 in Figure 3, the multiple-scale model increases the size of the central recirculation region and reduces the diffusion. At X/D = 2.5 (Fig. 4), augmentation of turbulence by the multiple-scale model smooths the axial velocity profile. In fact, the mean flow is almost fully recovered to the fully developed pipe flow at this location. Shown in Figure 5 is a comparison of the predicted central recirculation zone boundary using the k-ε models and the multiple-scale model with data of Roback and Johnson. The k-ε model, as well as two modifications, produces a shorter central recirculation zone. The prediction of the width and the length of the recirculation zone is much improved by the multiple-scale model. The recirculation zone shape, formed in Roback and Johnson's experimental setup, is of type 3 mentioned above. This type 3 shape is mimicked faithfully by the multiple-scale turbulence model. This feature is plotted in Figure 6(a) at X/D = 0.21 and X/D = 0.42. Also shown in Figure 6(c) are predictions of Sloan [17] of the same case using standard k-ε, Richardson number correction to k-ε, and a non-isotropic algebraic stress model, ASM. The multiple-scale obviously has the edge of predicting the "three cell" flow structure in the confined swirling flow.

Figure 7 compares radial profiles of mean tangential velocities at X/D = 0.833 and 2.5. The single-scale model is seen to have a more rapid decay of swirl component than the multiple-scale model at the upstream location. However, both models predict tangential velocity decay to a solid-body rotation prematurely, while the experimental data of Roback and Johnson persist in a combined vortex profile even at far downstream. The discrepancies between the calculations and measurements indicate the deficiency of isotropic eddy viscosity hypothesis used in this level of closure. This discrepancy is also shared by the non-isotropic algebraic stress model (ASM) prediction [6]. As indicated by Sloan et al., the failure at the downstream location probably has to be resolved by solving the full stress transport equations, with convective and diffusive terms, rather than the abbreviated ASM.

Shown in Figure 8 are predictions of turbulence intensity at several downstream locations. Both models follow the trend of experimental data fairly well except that the peak values are underpredicted. Multiple-scale model seems to have a more realistic presentation of the fluctuation near the wall region. Again, the higher level of turbulence intensities at the downstream region is that the kinetic energy contained by the transfer eddies (or small-scale eddies), k_t, is independent of the mean strain rate. Although the production of k_p is very small here, the production of k_t still persists.

Recently the sensitivity of the numerical prediction to the inlet boundary conditions has gained increased concern [11-14]. It is instructional to examine the response of the flow field to variations in turbulence quantities of inlet streams. Since the mean variable profiles are taken from experimental data, the uncertainty associated with mean field inlet boundary conditions would be minimal. The specification of turbulence quantities, such as k_p, k_t, ε_p and ε_t, on the other hand, is in doubt. Computations compared above were performed using "non-eqilibrium" spectral shape. In order to examine the effect of the assumed spectral shape of turbulence, calculations were made with "partially-eqilibrium" and "equilibrium" inlet spectra. In the partially-equilibrium spectrum, the kinetic energy is separated such that k_p = 0.7 k and k_t = 0.3 k. In the equilibrium case, both inlet ε_p and ε_t were set equal

to ε and the division of the energy spectrum is moved to high wave numbers such that only a very small portion of the turbulence kinetic energy is contained in k_t. As seen from Figures 9 and 10, the difference of mean flow field predictions between using non-equilibrium and partially-equilibrium initial spectra is not appreciable. The prediction starting with equilibrium spectral shape, however, shows substantial departure from that of non-equilibrium shape. The kinetic energy spectrum in most inlet planes of complex flows cannot be equilibrium. Thus, it is recommended that non-equilibrium or close to non-equilibrium spectral shape should be used to start the calculation.

IV. CONCLUDING REMARKS

Despite the fact that the proficiency of turbulence model predictions may be obscured by the influences of boundary conditions, numerical diffusion, grid system and oscillatory phenomena, significant benefits can be gained in elucidating the relative advantages of various turbulence model predictions. It is demonstrated in this study that the multiple-scale turbulence model exhibits great potential in swirling flow predictive capability. The preliminary success of the multiple-scale turbulence model stems from recognizing that the turbulence in swirling flow is highly non-spectral-equilibrium, and, that the different energy transfer rates for different eddies should be modeled separately. However, the multiple-scale turbulence model still adopts the isotropic eddy viscosity formulation. To take into account the anisotropy of the flow turbulence, full Reynolds Stress Model has to be used. Incorporation of the multiple-scale turbulence model, which takes into account the non-equilibrium spectral energy transfer rate and simplified Reynolds Stress Model, should pave a promising avenue for numerical modeling of swirling flows.

One last note is that although much research has to be aimed at improving predictive capabilities of current turbulence models, the development of the numerical efficiencies and accurate differencing schemes for validating and optimizing turbulence models should not be overlooked. More recent works [18-20] have been devoted to these developments. Also, fundamental experimental investigations including the detailed inlet boundary conditions measurements and characterization of the discharging flow from swirlers remain an absolute necessity for guiding and testing computational models.

REFERENCES

1. Rodi, W.: AIAA J., Vol. 20, 1982, p. 872.

2. Escudier, M. P., Bronstein, J., and Zehnder, N.: J. Fluid Mech., Vol. 98, 1980, p. 49.

3. Launder, B. E., Priddin, C. H., and Sharma, B. I.: J. Fluid Eng., Vol. 88, 1977, p. 231.

4. Rodi. W.: Proc. 2nd Symp. on Turbulent Shear Flows, 1979, p. 10.37-10.42.

5. Chen, C. P.: Commu. in App. Nume. Method., in press, 1985.

6. Sloan, D. G., Smoot, L. D., and Smith, P. J.: Modeling of Swirl in Turbulent Flow Systems. Paper presented, Combustion Inst. Spring Technical Meeting, April 22-23, Southwest Research Institute, 1985.

7. Gupta, A. K., Lilley, D. G., and Syred, N.: Swirl Flows. Abacus Press, 1984.

8. Hanjalic, K., Launder, B. E., and Schiestel, R.: in Turbulent Shear Flow II, 1980, p. 36.

9. Chen, C. P.: Multiple-Scale Turbulence Modeling in Internal Flows. 3rd SSME CFD Workshop, NASA-MSFC, manuscript submitted to Phys. Fluids, 1985.

10. Roback, R. and Johnson, B. V.: NASA CR-168252, 1983.

11. Leschziner, M. A. and Rodi, W.: AIAA J., Vol. 22, 1984, p. 1742.

12. Sturgess, G. J., Syed, S. A., and McManus, K. R.: AIAA paper 83-1263, 1983.

13. Ramos, J. I.: AIAA J., Vol. 22, 1984, p. 846.

14. Lilley, D. G.: NASA CR-3869, 1985.

15. Gosman, A. D. and Ideriah, F. J. K.: TEACH-T, Dept. of Mech. Eng., Imperial College, London, 1976.

16. Dixson, T. F., Truelove, J. S., and Wall, T. F.: J. Fluid Eng., Vol. 105, 1983, p. 197.

17. Sloan, D. G.: Modeling of Swirl and Heterogeneous Char Combustion in Pulverized Coal Systems. Ph.D. Thesis, Brigham Young Univ., 1985.

18. Syed, S. A. and Chiapetta, L. M.: AIAA paper 85-0057, 1985.

19. Sturgess, G. J. and Syed, S. A.: AIAA paper 85-0060, 1985.

20. Vanka, S. P.: AIAA paper 85-0141.

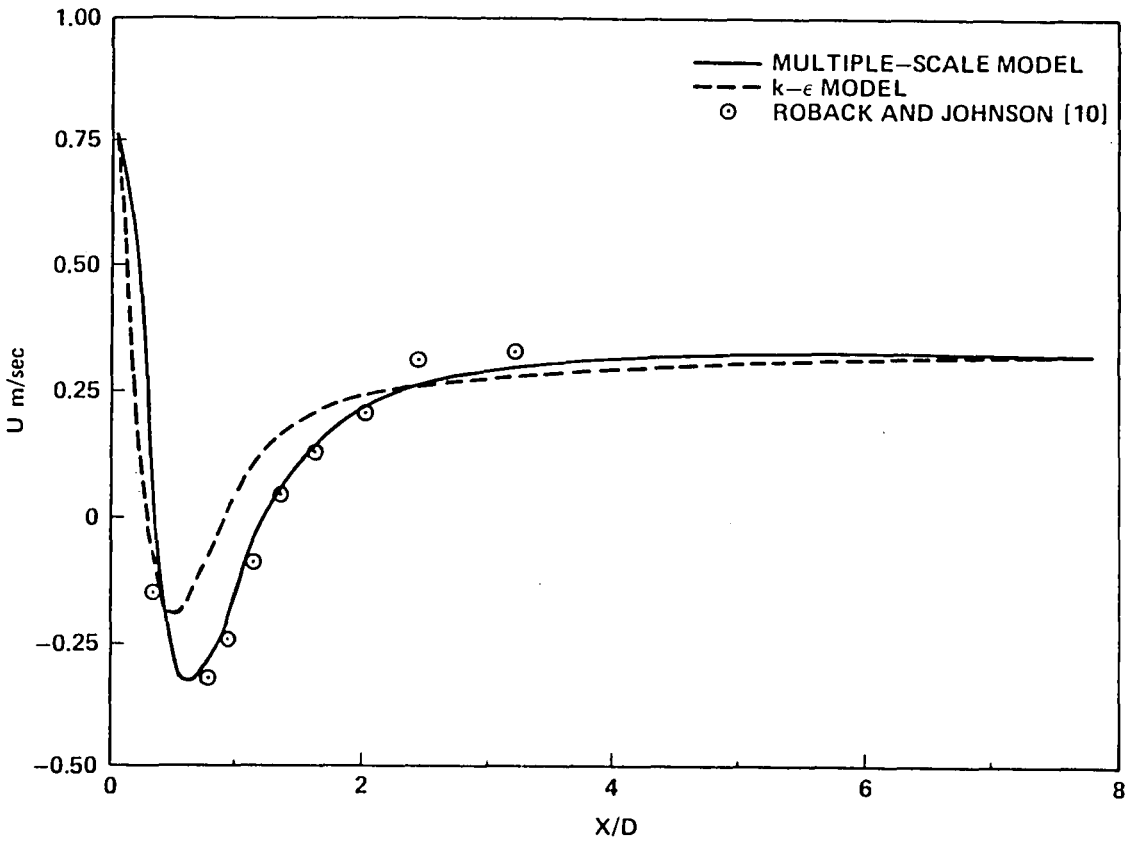

Figure 1. Decay of mean axial centerline velocity.

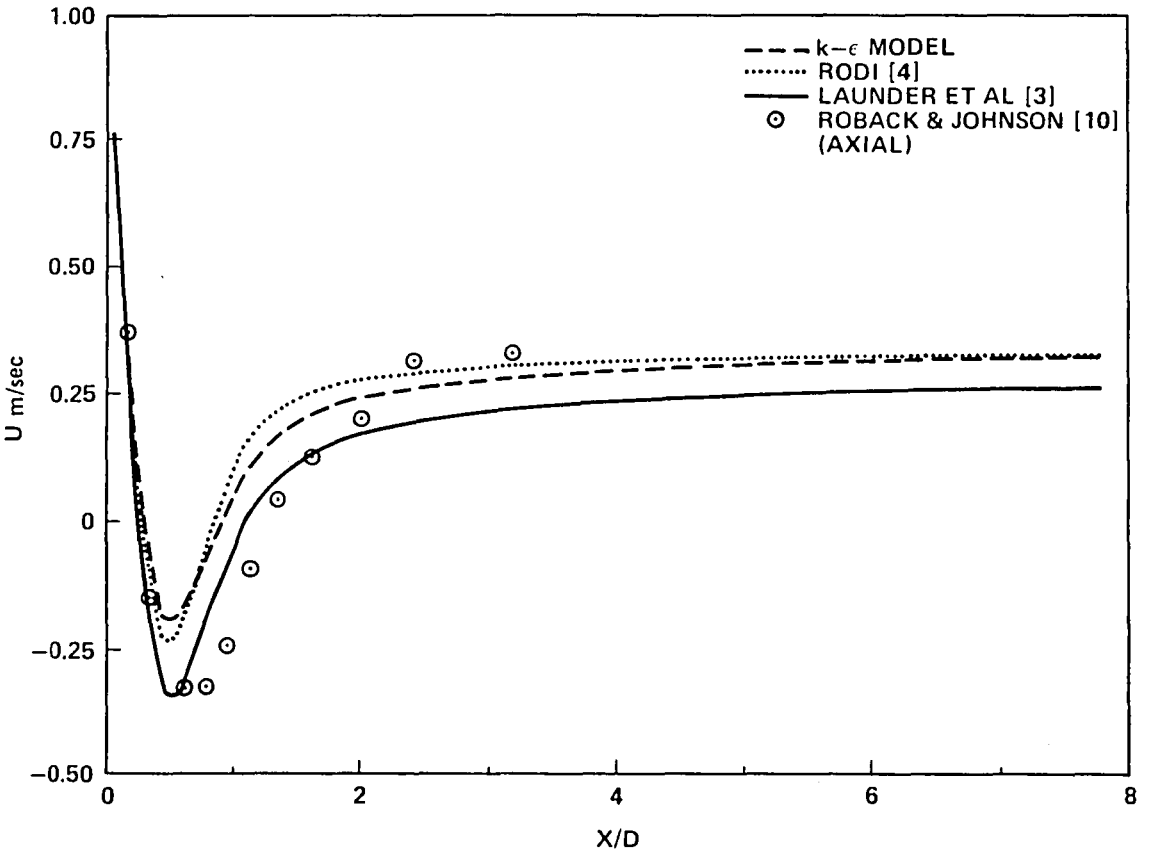

Figure 2. Decay of mean axial centerline velocity, taken from [5].

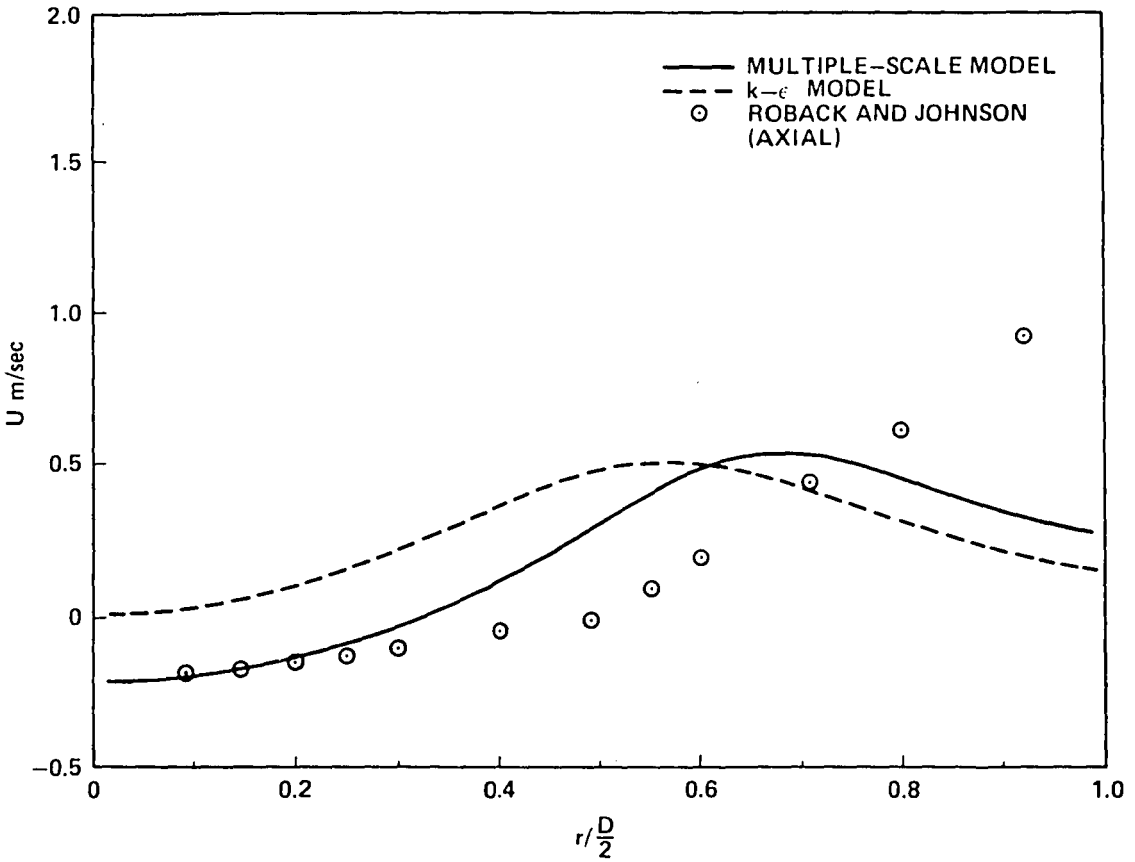

Figure 3. Axial mean velocity profiles at X/D = 0.833.

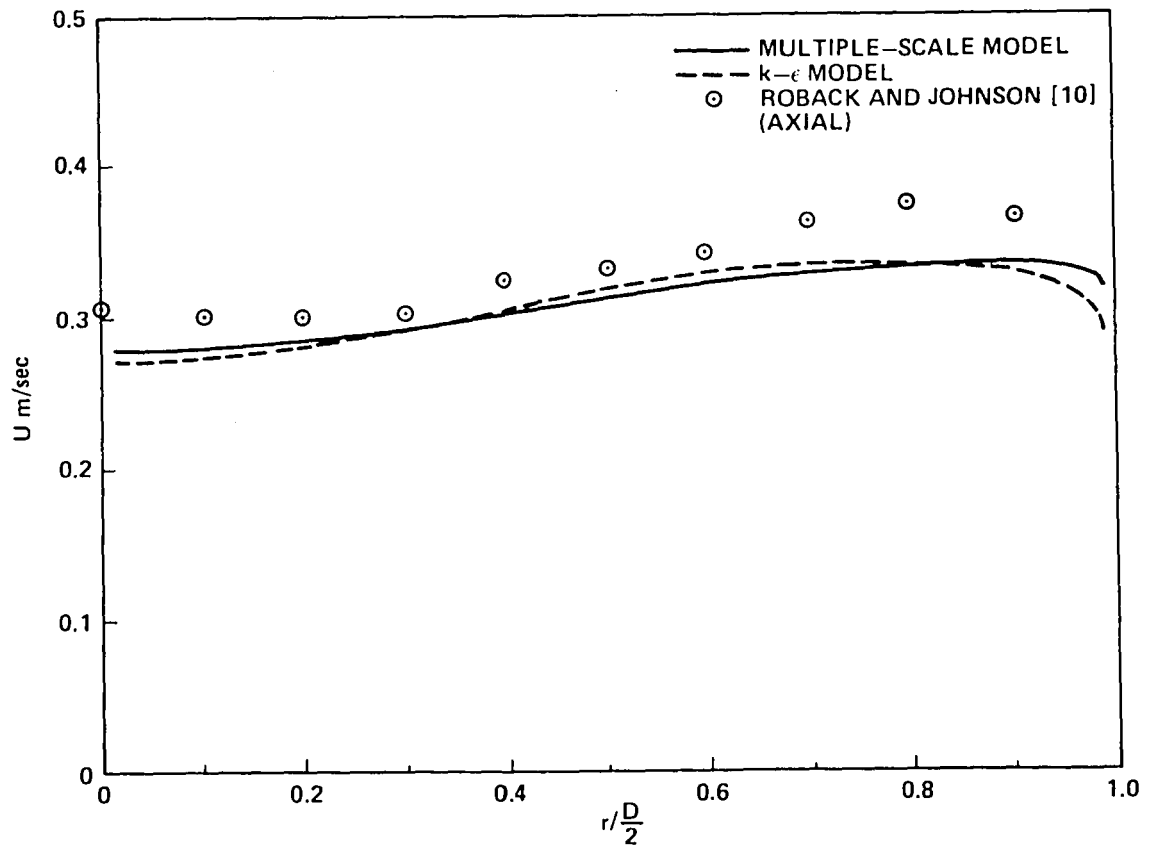

Figure 4. Axial mean velocity profiles at X/D = 2.5.

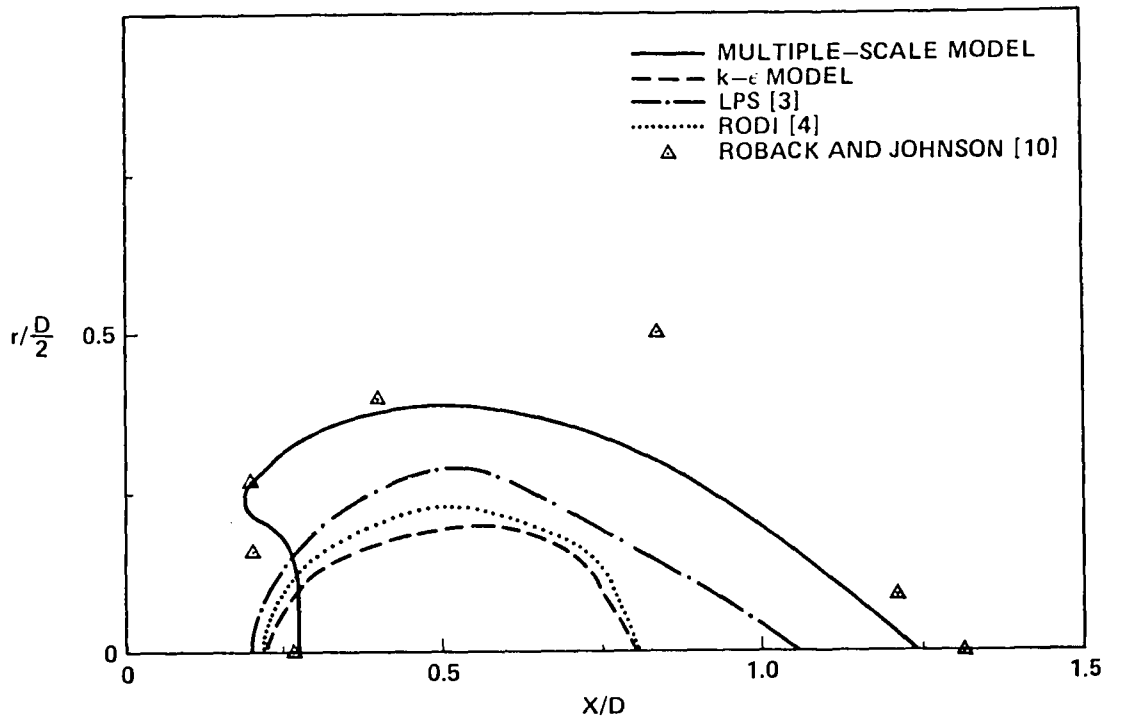

Figure 5. Envelope of the central recirculation zone.

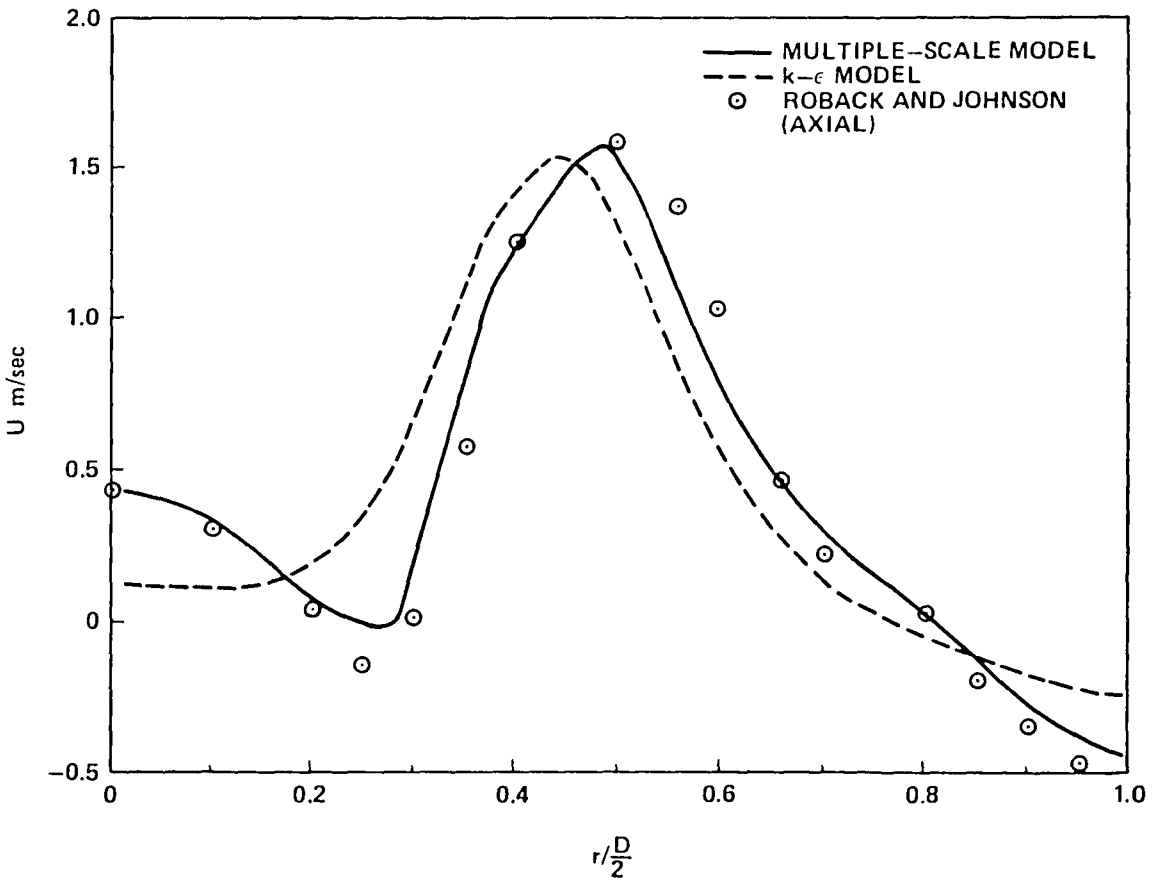

Figure 6(a). Axial mean velocity profile at X/D = 0.21.

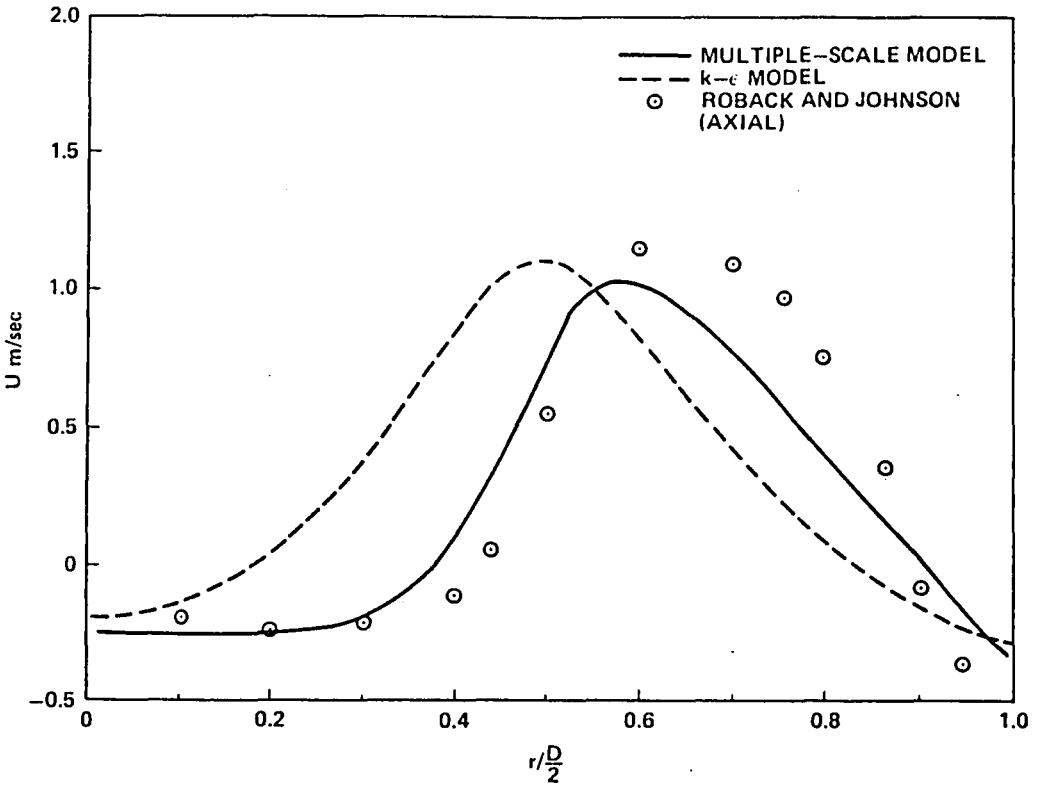

Figure 6(b). Axial mean velocity profile at X/D = 0.42.

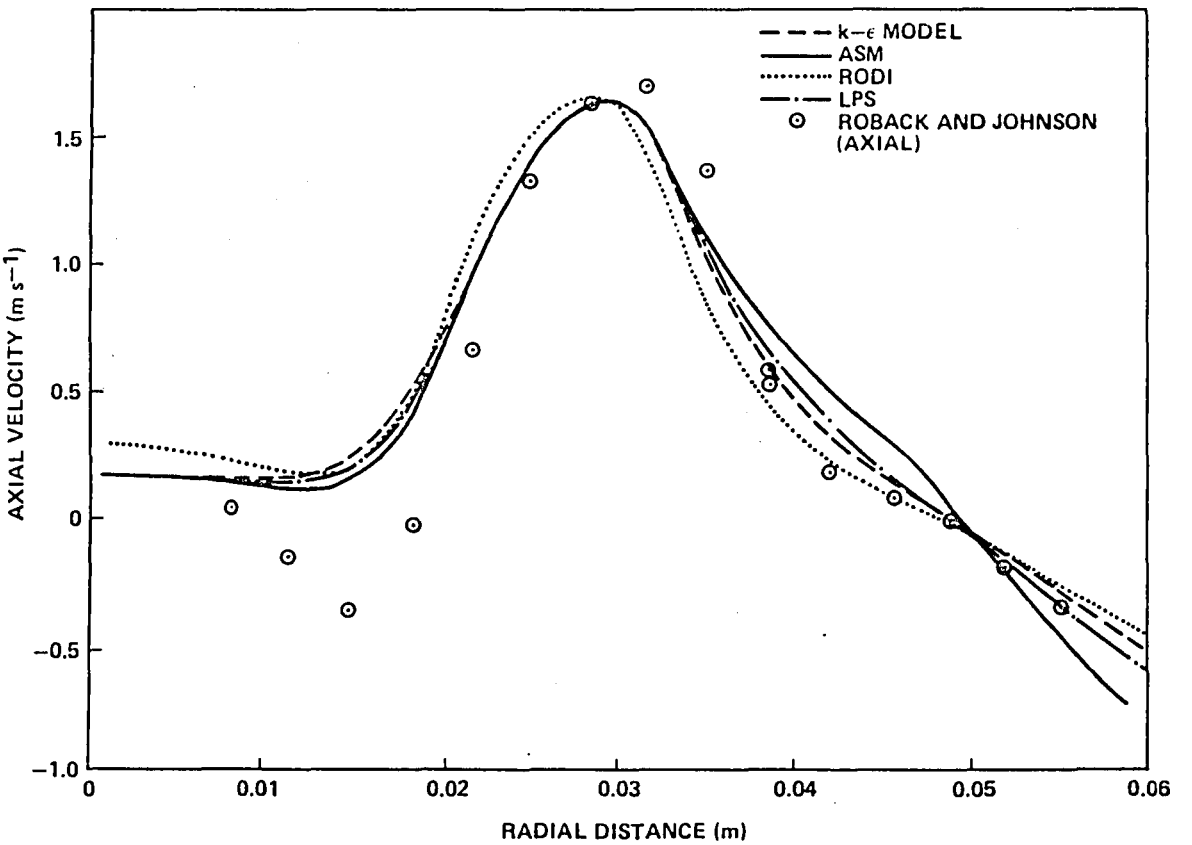

Figure 6(c). Axial mean velocity profile at X/D = 0.21, taken from [17].

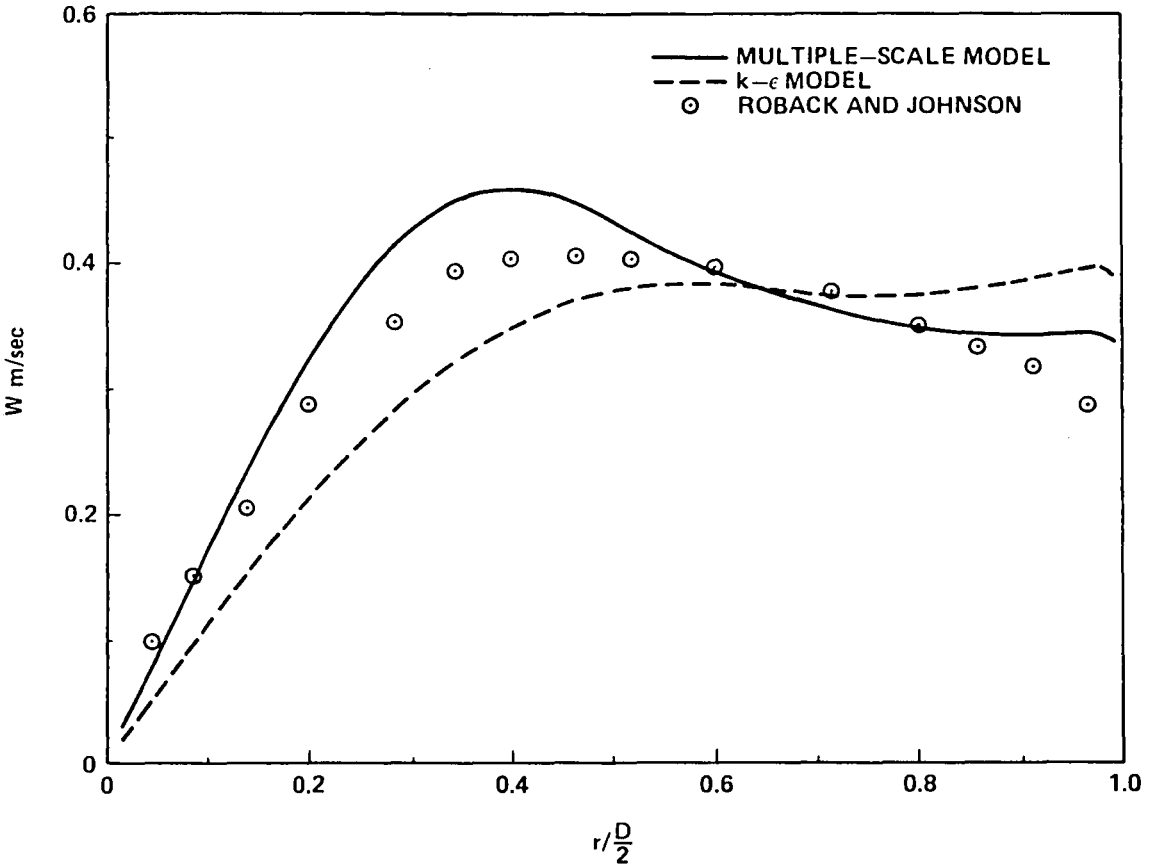

Figure 7(a). Tangential mean velocity profile at X/D = 0.833.

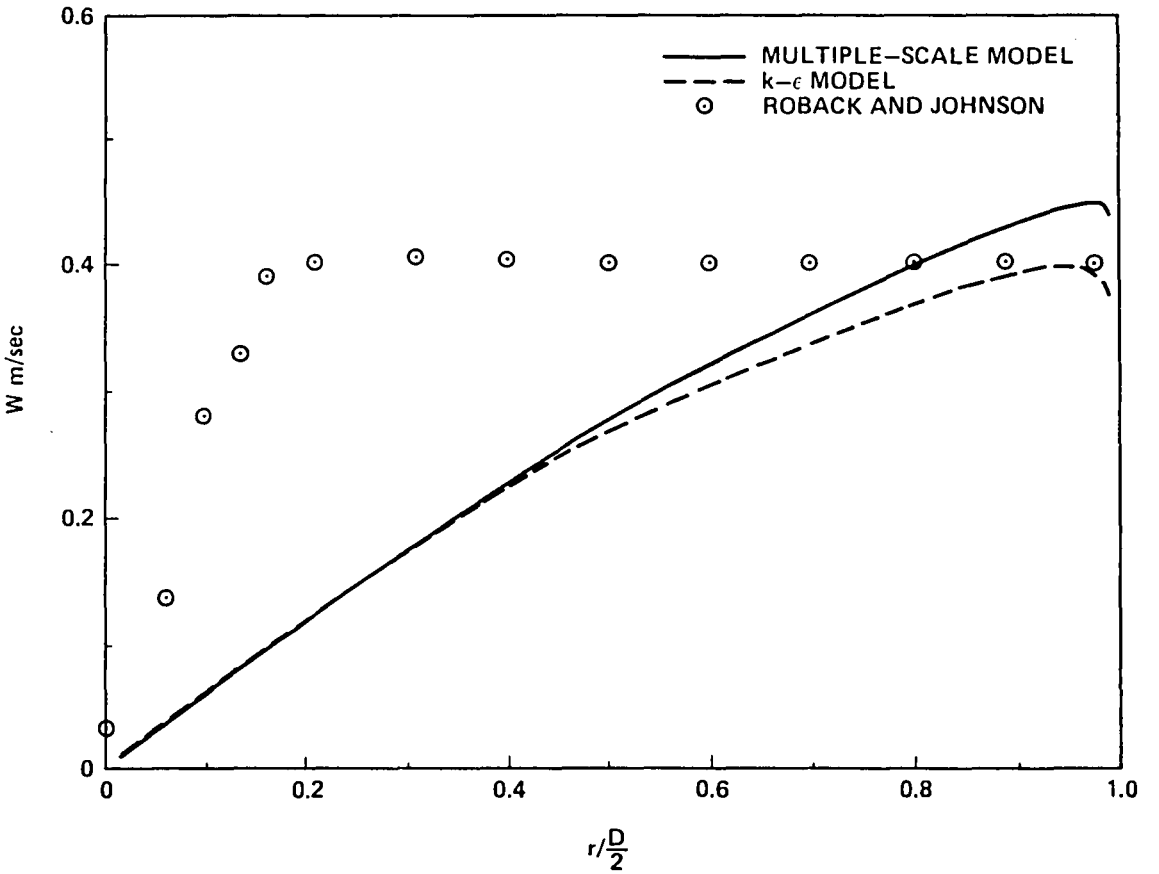

Figure 7(b). Tangential mean velocity profile at X/D = 2.5.

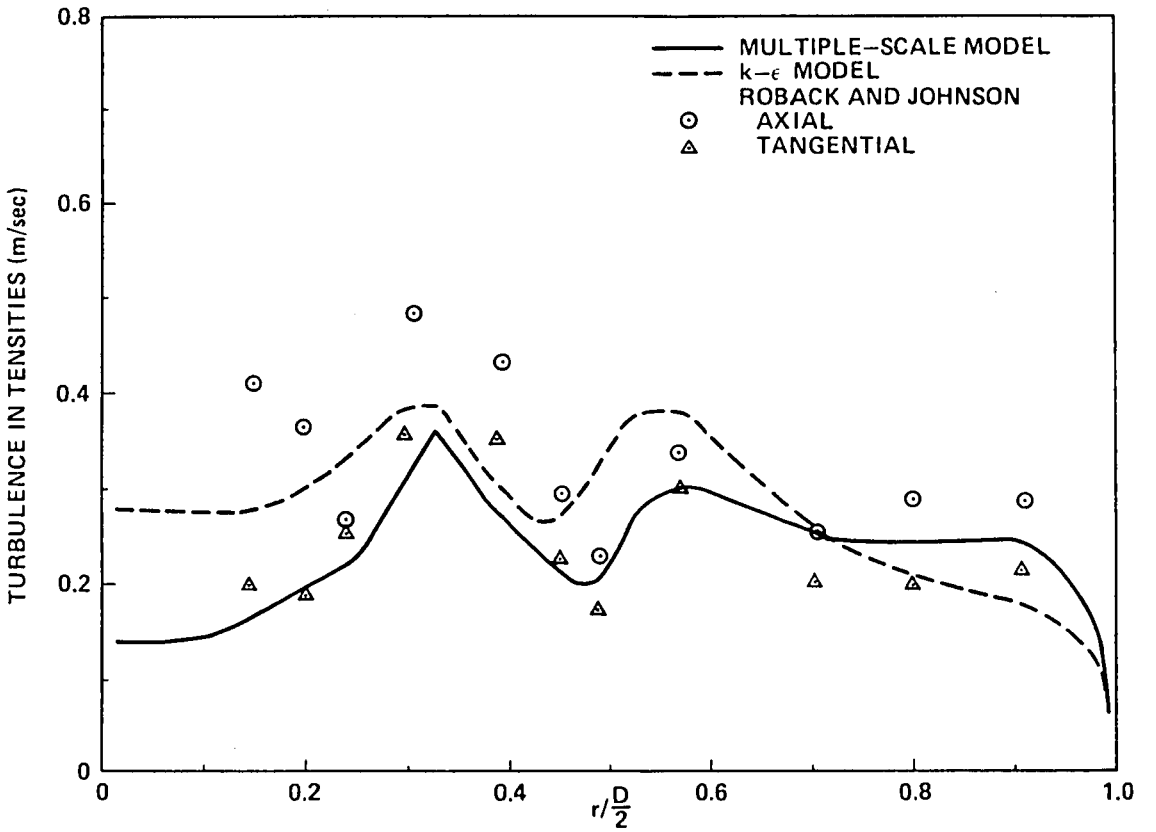

Figure 8(a). Turbulence intensity profile at X/D = 0.21.

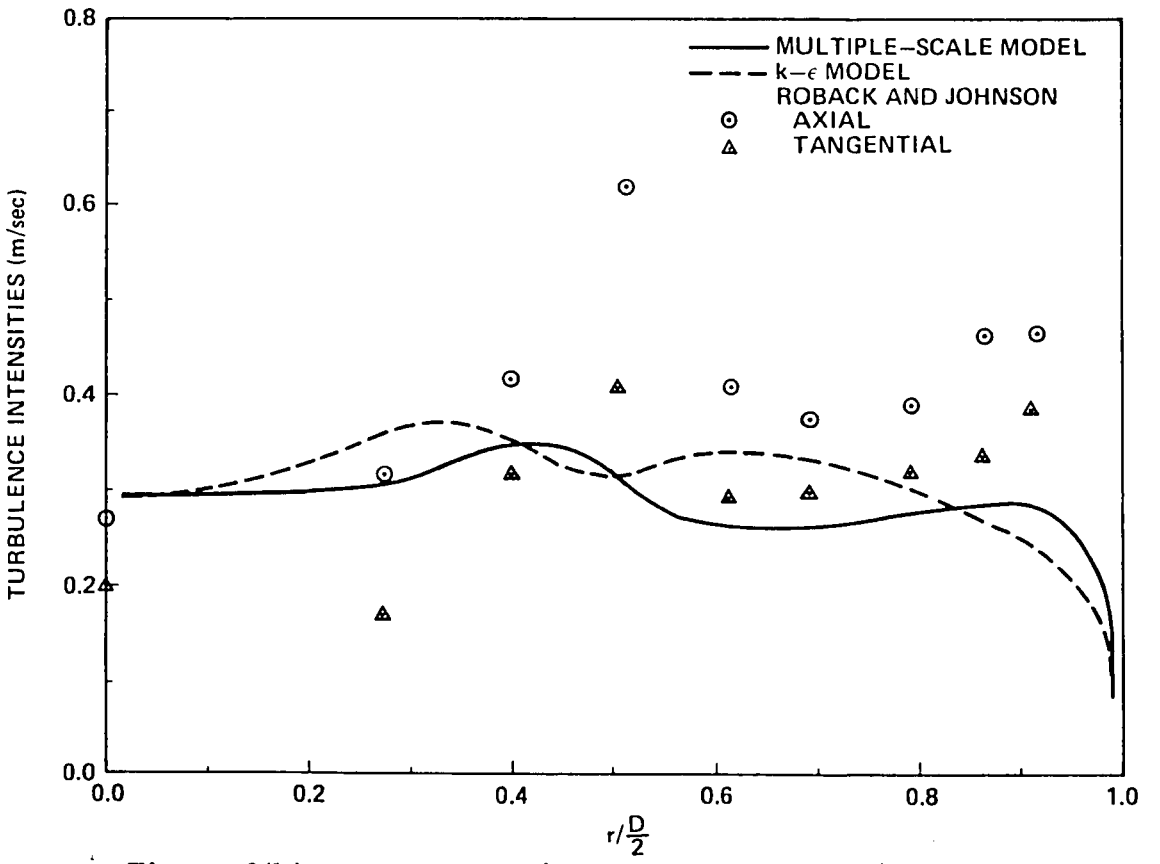

Figure 8(b). Turbulence intensity profile at X/D = 0.42.

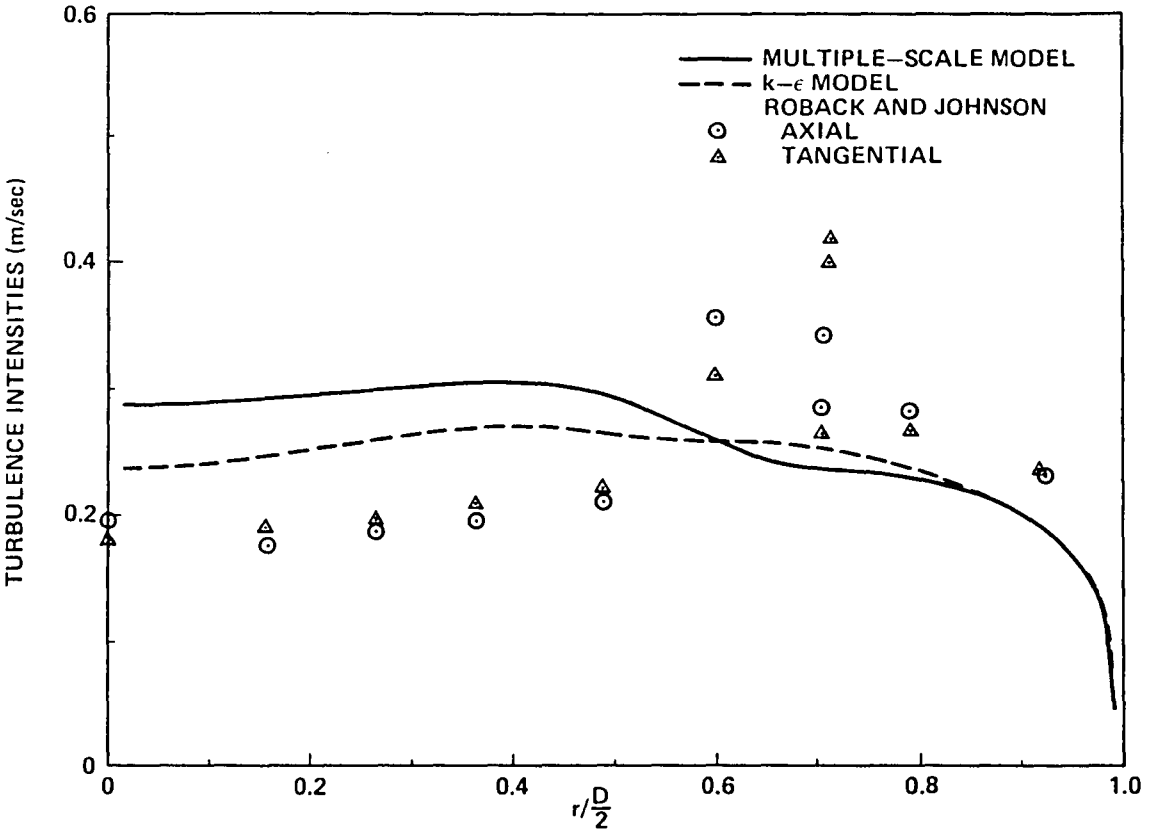

Figure 8(c). Turbulence intensity profile at X/D = 0.833.

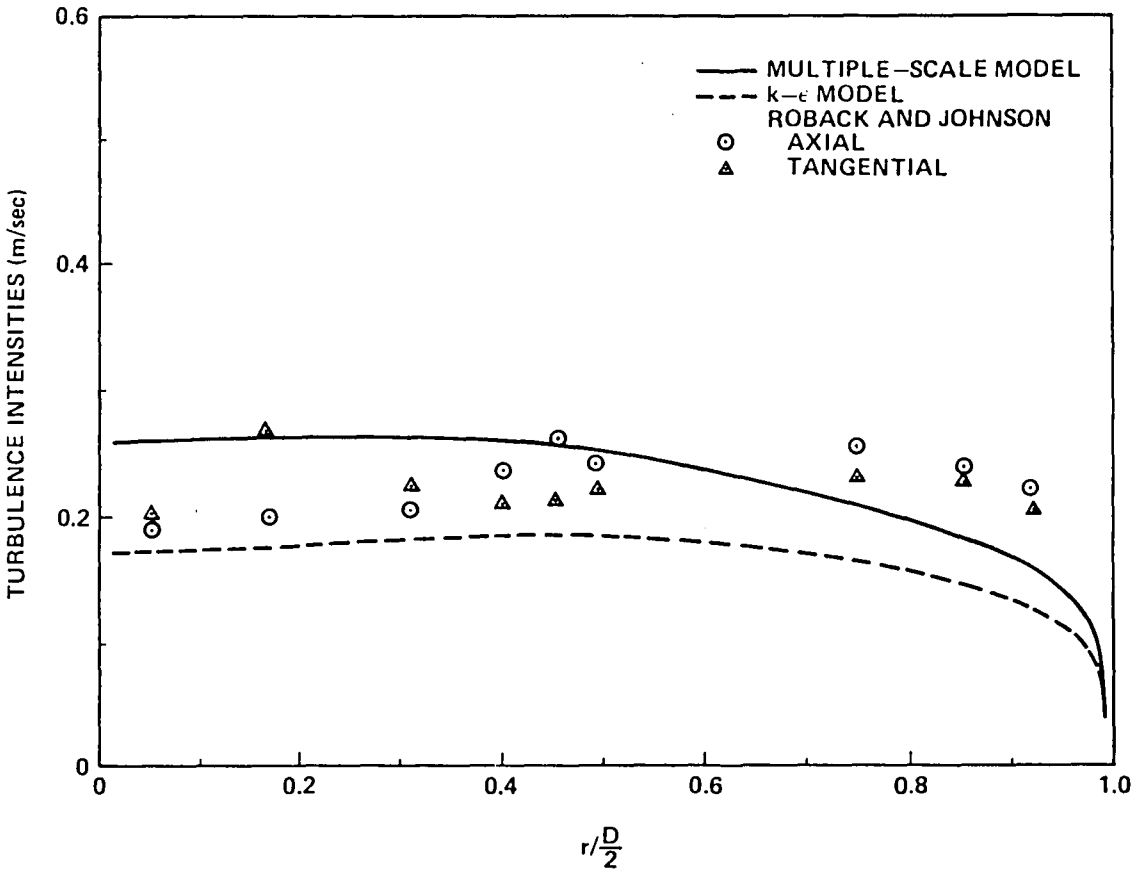

Figure 8(d). Turbulence intensity profile at X/D = 1.25.

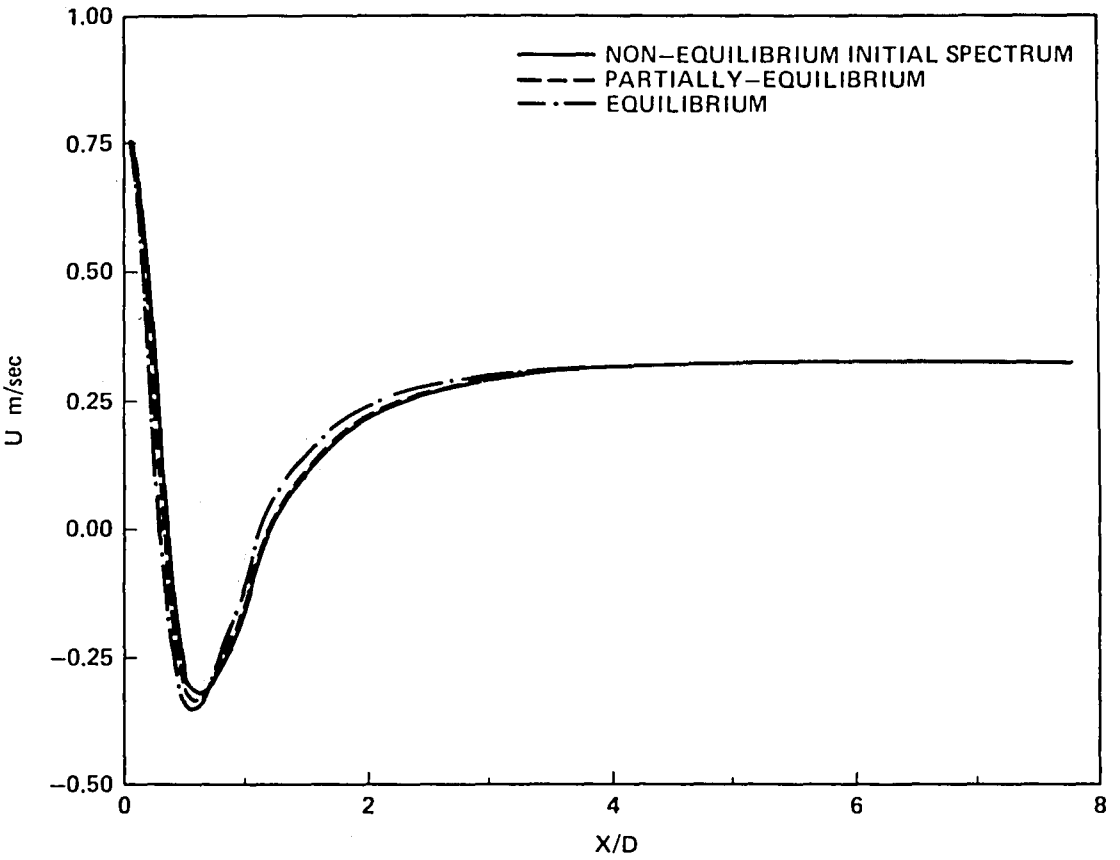

Figure 9. Effects of initial spectrum shape on the flow.

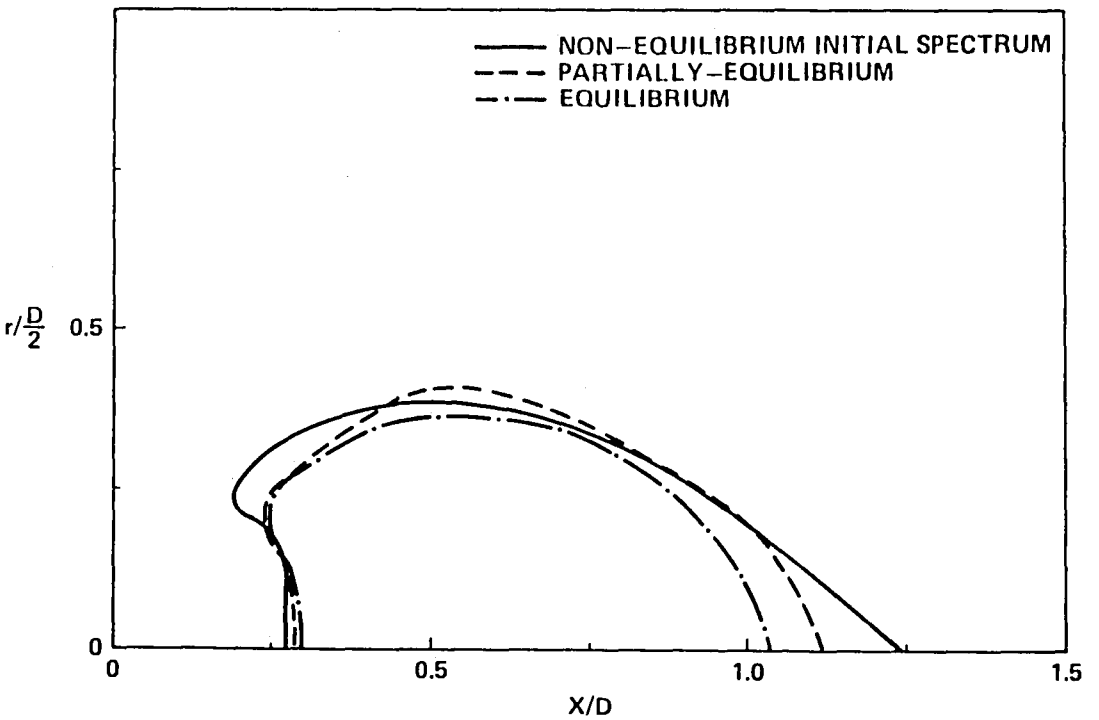

Figure 10. Effects of initial spectrum shape on the centerline velocity.

APPROVAL

CONFINED SWIRLING JET PREDICTIONS USING A
MULTIPLE-SCALE TURBULENCE MODEL

By C. P. Chen

The information in this report has been reviewed for technical content. Review of any information concerning Department of Defense or nuclear energy activities or programs has been made by the MSFC Security Classification Officer. This report, in its entirety, has been determined to be unclassified.

G. F. McDONOUGH
Director, Systems Dynamics Laboratory

☆U.S. GOVERNMENT PRINTING OFFICE 1985—544-048/20010

End of Document